MORPHOLOGY AND MECHANICAL BEHAVIOR OF A NATURAL COMPOSITE: THE FLAX FIBER

Charlet Karine*, Jernot Jean-Paul*, Gomina Moussa*
Baley Christophe, Bizet Laurent***, Bréard Joël*****
***CRISMAT, Caen, France, **L2PIC, Lorient, France, *** LMPG, Le Havre, France**

Keywords: *flax, morphology, mechanical properties, natural composite material, microfibril angle*

Abstract

In this paper, we present some relationships between the tensile mechanical properties and the microstructural features of a natural composite material: the flax fiber. The beginning of the stress-strain curve of a flax fiber upon tensile loading appears markedly non-linear. The hypothesis of a progressive alignment of the cellulose microfibrils with the tensile axis provides a quantitative explanation of this departure from the linearity. This hypothesis is confirmed by a similar analysis of the behavior of cotton fibers. Besides, it has long been recognized that the natural character of flax fibers induces a large scattering of their mechanical properties. This scattering is shown not to be ascribed to the pronounced cross-section size variation observed along the fiber profiles.

1 Introduction

A flax fiber is a biodegradable natural composite material which exhibits good specific mechanical properties. Consequently, this fiber is foreseen as a reinforcement material in polymeric based structural composites in replacement of the largely used E-glass fibers.

On one hectare of soil, about 1.5 tons of long flax fibers, entirely devoted to the textile industries, and 1.2 tons of short flax fibers, 80% of which is used in the textile industries and 20% in composite materials, can be produced [1]. During the year 2005 in France, 81 500 hectares were cultivated with flax, which means that the capacity to produce short and long fibers for material composites was 220 000 tons. As a comparison, French glass industries produced about 295 000 tons of “technical glass fibers” during the same year [2]. This means that almost all the glass fibers produced could have been replaced by flax fibers. Nevertheless, before using this fiber as a reinforcement for composite materials, its microstructural and mechanical properties have to be well understood.

After a brief description of the flax fiber structure, its mechanical properties are given in the first part of the paper. Then, the relationships between the mechanical properties and the microstructure are discussed in the second part.

2 Structure of flax

The multilayer composite structure of the flax fiber is presented in figure 1. The fibers are located within the stems, between the bark and the xylem. Around twenty bundles can be seen on the section of a stem and each bundle contains between ten and forty fibers linked together by a pectic middle lamella. Each fiber is made of a thin external layer, called the primary cell wall, and a thick secondary cell wall, which is divided into three layers (S1, S2 and S3).

The cell walls are made of cellulose microfibrils laid in spirals around the fiber axis and embedded in a pectic matrix. In the secondary cell wall, the angle between the microfibrils and the longitudinal axis (called the “microfibril angle”) is about 10° [3-5]. In a flax bundle, the weight fraction of cellulose has been evaluated at 65-75%, the one of non-cellulosic polymers (i.e. pectins, hemicelluloses and lignin) at 20-25% and the one of water at 8-10% [6]. Considering the microstructural arrangement, the cellulose microfibrils act as the reinforcement of the pectic matrix and the interface between these two materials is mainly composed of hemicelluloses [7].

The development of fibers is directly linked to the growth of the stem, between March and July. It can be separated into three stages: the first stage corresponds to the elongation of the thin primary cell wall, from a few millimeters to several centimeters. The second stage begins with the centripetal synthesis of the secondary cell walls: first

the S1 layer, then the main S2 layer and lastly the S3 layer. Growth is complete when the fiber is mature. During the lifetime of a cell, the center of the fiber is filled with the cytoplasm; after the death of the cell, this empty space is called “lumen”. Its section, which depends both on the perimeter of the primary cell wall and on the thickness of the cell walls, represents less than 10% of the entire fiber section [8].

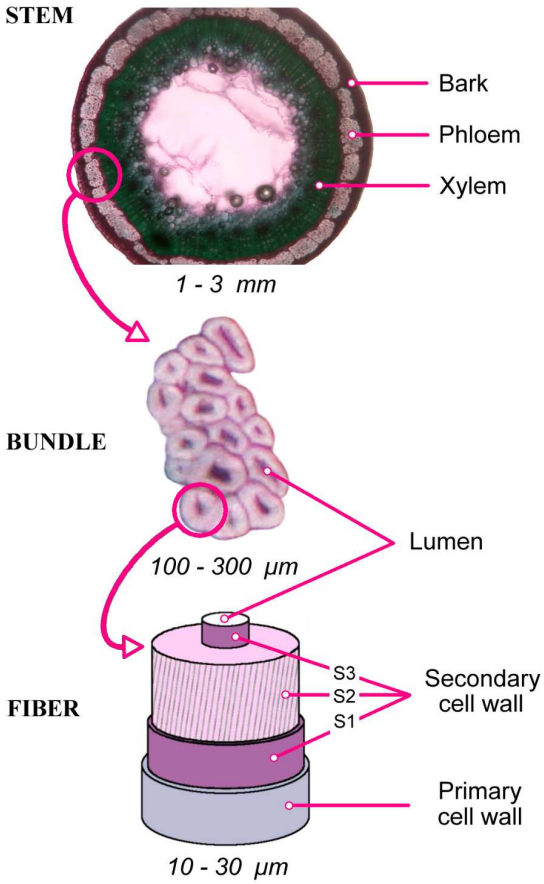

Fig 1. Structure of flax: from the stem to the fiber

The extraction of fibers from the stem is achieved in several steps. At first, the flax is dew-retted. This means that the stems are pulled up and laid on the ground for six to eight weeks so that natural micro-organisms ingest the pectic cement and isolate the bundles from the xylem and the bark. Then, the stems are mechanically scutched in order to eliminate shives and short fibers. At last, the long tows can be hackled to separate the bundles, align the fibers and form a continuous tape. This tape can then be manually or enzymatically treated to extract the single fibers which are the subject of the present study.

3 Tensile testing of flax fibers

Tensile tests have been carried out on single flax fibers using a universal MTS-type tensile testing machine equipped with a 2N capacity load cell. The accuracy of the crosshead displacement measurements is about 1 µm [9]. The mechanical properties were determined according to the NFT 25-704 standard by taking into account the compliance of the loading system (previously estimated by tensile testing E-glass fibers).

As the length of the flax fibers varies from a few millimeters to several centimeters, with a mean length around 30 mm [6], a gauge length of 10 mm has been chosen. A schematic representation of the tensile testing protocol is given in figure 2.

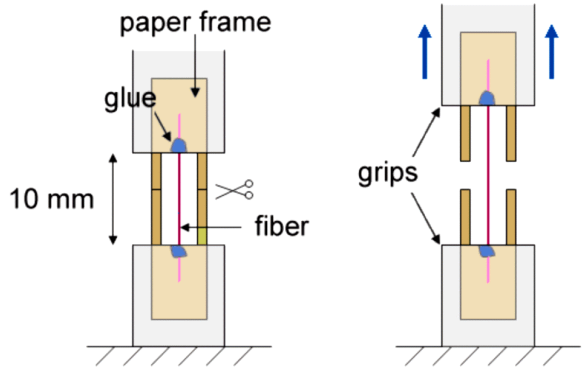

Fig. 2. Schematized testing protocol of a flax fiber

Before the tensile test, the fiber is glued on a paper frame. The fiber diameter is estimated as the average of three optical measurements along the fiber. Then the top and bottom edges of the frame are clamped into the grips and its sides are cut. The fiber is tested in tension at a constant crosshead displacement rate of 1 mm/min until it fails. About two hundred single fibers have been tested in these conditions.

A typical stress-strain curve of a flax fiber is shown in figure 3. It displays three different behaviors spanning three successive zones. A first linear zone corresponds to the beginning of the fiber loading. A curved trend is observed in the next zone. The third zone corresponds to a linear behavior before the brittle failure of the fiber. The Young's modulus is calculated from the slope measured in this last region, whereas some authors recommend considering the total slope of the stress-strain curve [10].

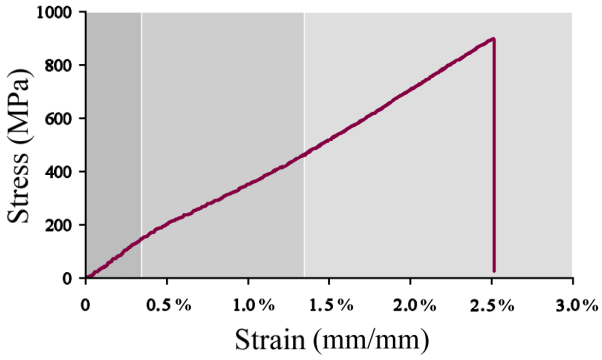

Fig. 3. Typical tensile stress-strain curve of a flax fiber

The Young's modulus, the strength and the failure strain have been calculated for each tested fiber. The mean experimental results are given in table 1 where they are compared with literature data [9,11].

Table 1. Mean mechanical properties and mean diameter of tensile tested flax fibers (line 1). The two bottom lines correspond to literature data ([9] line 2 and [11] line 3)

E (GPa)	σ_r (MPa)	A_r (%)	d (µm)
56 ± 28	1099 ± 558	2.3 ± 0.9	17.5 ± 4.2
54 ± 15	1339 ± 486	3.3 ± 0.8	23.0 ± 5.7
60 ± 10	700 ± 200	2.8 ± 1.3	19

These raw mean results can be refined by an analysis of the mechanical properties as a function of the fiber size. In figure 4 are displayed the evolutions of (a) the strength and (b) the Young's modulus as a function of the fiber diameter. The two striking points are the great scattering of the results and a downward trend when the fiber diameter increases. In a first approach, the scattering can be simply explained by the natural character of the fibers whose internal structure can differ noticeably according to the growing conditions, the variety, or the location in the stem… The decrease of the strength can be understood by considering the numerous defects existing in a natural fiber. Many authors have already applied the Weibull statistics successfully to link the failure probability to the amount of defects and thus to the fiber dimensions [12-14]. But the decrease of the Young's modulus when the fiber diameter increases, already emphasized in the literature [9,12], cannot be easily explained since the stiffness is an intrinsic material property and should be independent of the sample size.

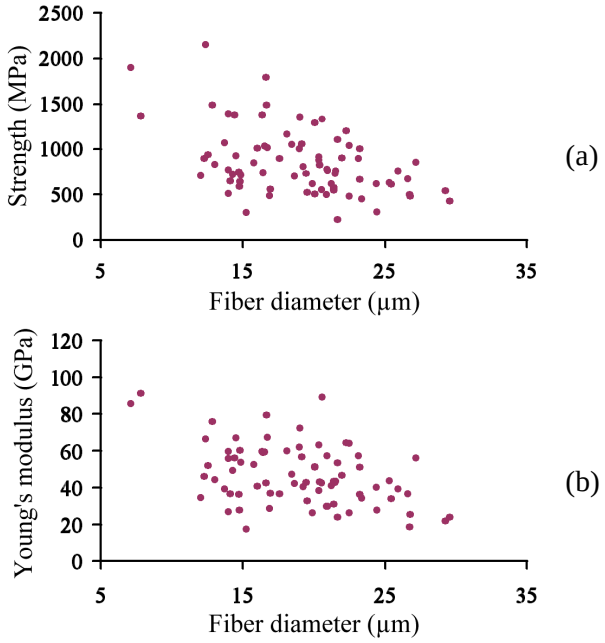

Fig. 4. (a) Strength and (b) Young's modulus of flax fibers as a function of their diameters

Three main characteristics of the flax fiber tensile behavior emerge from these experiments: the first one is the non-linearity of the beginning of the stress-strain curve; the second one concerns the scattering of the results; the third one is the decrease of the mechanical properties as a function of the fiber diameter. These points are investigated in the following sections by taking into account the specific morphology of the flax fibers.

4 Deformation behavior of a flax fiber

The knowledge of the internal structure of a flax fiber allows for the elaboration of an interpretation of its deformation mechanisms. The first linear zone of the stress-strain curve would correspond to a global loading of the cell walls. Then, the curved zone could be associated to a visco-elasto-plastic deformation of the amorphous parts of the fiber together with an alignment of the cellulose microfibrils with the fiber axis. Finally, after this rearrangement, the third linear zone could be characteristic of the elastic deformation of the microfibrils. During this last stage, the interphases between the different layers of the fiber or between the cellulose microfibrils are expected to shear, which would explain that the slope in this zone of the curve does not reach the level of the Young's modulus of the cellulose microfibrils, estimated at 134 GPa [15].

This interpretation is corroborated by literature data. The hypothesis of a visco-elasto-plastic deformation is validated by the existence of hysteresis loops and residual deformation during fiber cyclic axial tension tests [16]. This residual deformation would be mainly due to the deformation of the amorphous matrix. Moreover, in 1941, an optical observation of flax fibers in polarized light allowed the arrangement of the microfibrils within a "fresh" fiber, i.e. free of tension, to be compared with the one within a "manually stretched out" fiber [17]. A change in the orientation of the microfibrils after elongation of the fiber clearly appears. This reorientation may be possible thanks to the shear of the amorphous pectic zones within the cell walls, as already mentioned in the case of celery collenchyma [18].

Besides, when the two hundred tensile curves are superimposed, the beginning of the third linear zone before the rupture corresponds to a mean deformation of 1.4% ± 0.7%. This deformation can be simply linked to the spiral angle of the cell wall reinforcement, as explained in figure 5.

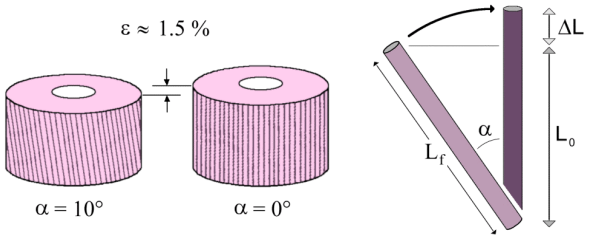

Fig. 5. Schematic representation of the microfibrils rearrangement

Let L_f be the length of a microfibril which initially forms an angle α with the fiber axis. The tension of the fiber brings about a change in the orientation of the microfibrils and a corresponding fiber lengthening ΔL :

$$\Delta L = L_f - L_0 = L_0\left(\frac{1}{\cos\alpha} - 1\right) \qquad (1)$$

i.e. a global deformation equal to (in mm/mm) :

$$\varepsilon = \ln\left(1 + \frac{\Delta L}{L_0}\right) = -\ln(\cos\alpha) \qquad (2)$$

Using Eq. 2, a deformation of 1.4% ± 0.7% (see figure 6a) corresponds to an angle α of 9.6° ± 2.5°. The distribution of the microfibril angles obtained by this calculation is shown in figure 6b. These microfibril angles are in the range of those already observed for flax fibers [3-5] mainly by RX analysis.

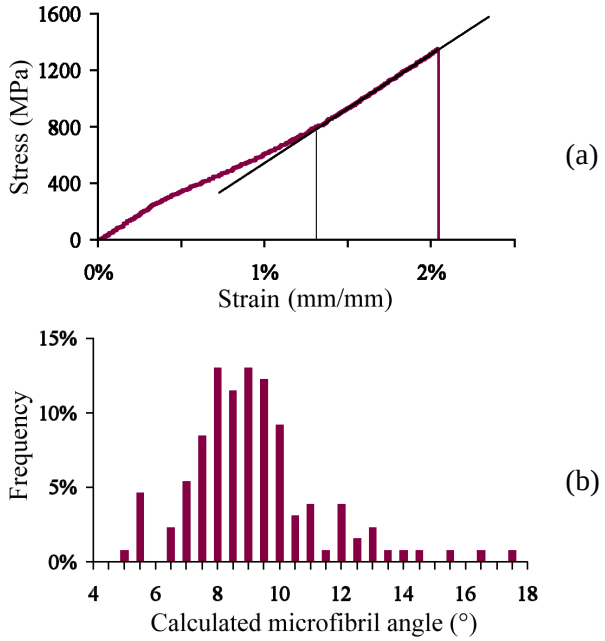

Fig. 6. Flax fibers: (a) tensile stress-strain curve; (b) histogram of the calculated microfibril angles

In order to confirm the relationship between the deformation at the beginning of the third linear zone and the microfibril angle, the protocol used to test flax fibers has been applied to cotton fibers which exhibit a higher spiral angle than flax fibers.

According to the literature, the initial orientation of the microfibrils within the cell walls of cotton fibers is estimated at 25° [19]. It must be noted that, for some authors, the microfibril angle depends on the ripeness of the fiber (from 1° for young fibers to 35° for mature fibers) [20] while for other ones it depends on the part of the cell wall considered (45° for the external S2 layer and 0° for the internal S2 layer) [21].

The same tensile tests as for flax fibers have been carried out on about sixty cotton fibers. A typical stress-strain curve of a cotton fiber is presented in figure 7a. As for a flax fiber, this curve exhibits three different zones. The beginning of the last linear zone corresponds to a mean deformation of 5.7% ± 2.7% which gives, by applying Eq. 2, a microfibril angle of 19.2° ± 4.6°. The distribution of the microfibril angles for cotton fibers is given in figure 7b.

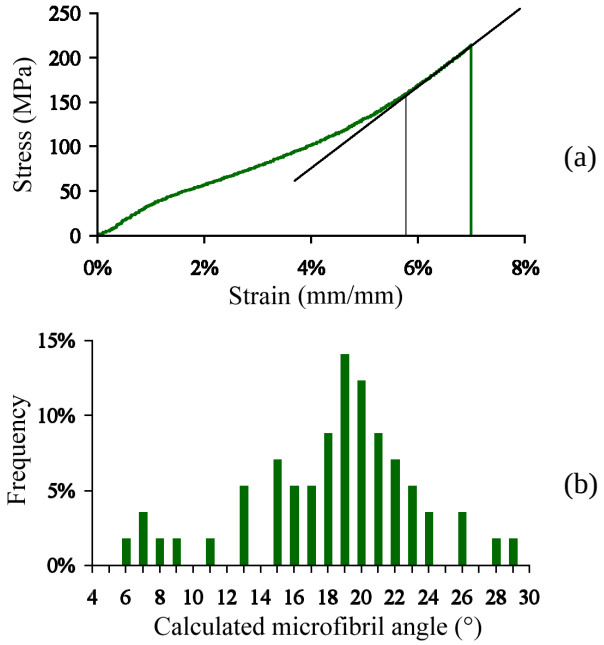

Fig. 7. Cotton fibers: (a) tensile stress-strain curve; (b) histogram of the calculated microfibril angles

For both cotton and flax fibers, the mean value of the calculated microfibril angle is not far from the usual values found for these fibers. Moreover, it seems from the literature that the microfibril angle is better defined for the flax fibers than for the cotton fibers. This is well reflected by the bar charts of the figures 6 and 7 in which the range of the microfibril angles is much wider for the cotton fibers than for the flax fibers.

Considering these results, it seems that the hypothesis expressed at the beginning of this section is realistic. For both flax fibers and cotton fibers, the non-linear region of the stress-strain curve can be associated to a visco-elasto-plastic deformation of the amorphous parts of the fiber and to an alignment of the cellulose microfibrils with the fiber axis since the deformation induced during a tensile test before the elastic behavior almost corresponds to the disappearance of the microfibril angle.

5 Fiber profiles

The authors had already tried to explain the scattering and the decrease of the mechanical properties of flax fibers (Hermès variety) as a function of the fiber diameter by the internal porosity of each fiber measured from cross-section areas [8]. This attempt turned out to fail as the porosity, estimated at 6.8% ± 3.5%, was almost independent of the fiber diameter and could not explain satisfactorily neither the scattering of the mechanical properties nor their decrease as a function of the fiber diameters.

Consequently, further observations on the fiber sizes have been carried out using a Hitachi S-3000N scanning electron microscope. The fiber size is no longer evaluated from a cross-section but its diametral profile is measured by inspecting it on its entire length. The observations made along about twenty fibers led to the conclusion that the fiber size varies considerably as a function of the location of the observation field. For some fibers the diameter has even been found to triple within a few millimeters. This is illustrated in figure 8 in which five micrographs of a 15 mm long fiber taken at different abscissae are presented. The entire profile of this fiber is given in figure 9.

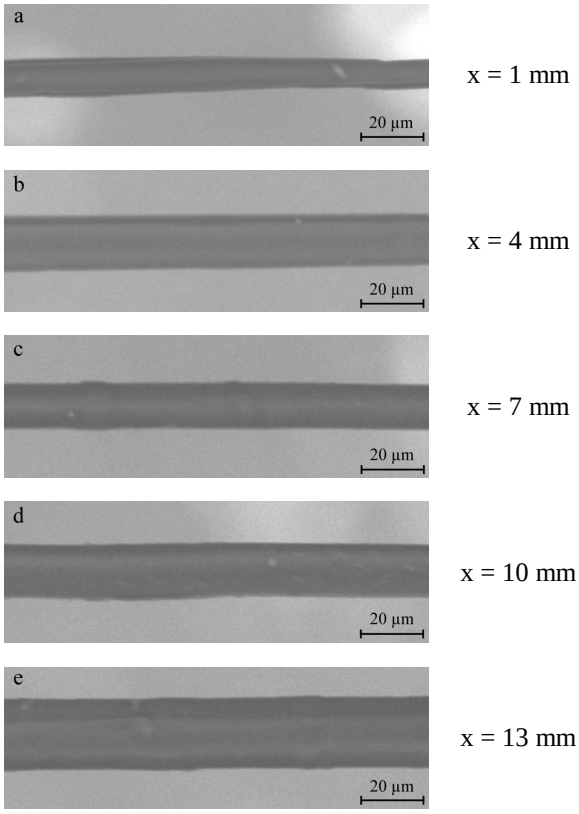

Fig. 8. SEM micrographs of a flax fiber (left) and their corresponding abscissa (right)

The notion of “fiber diameter” has then to be considered with caution: even for a single fiber, only a mean size can be defined. Moreover, this variation of dimensions within a single fiber could explain the scattering of the mechanical properties, since the size used to calculate the Young's modulus or the strength of a fiber is likely to differ from the size of a fiber at the location of its failure.

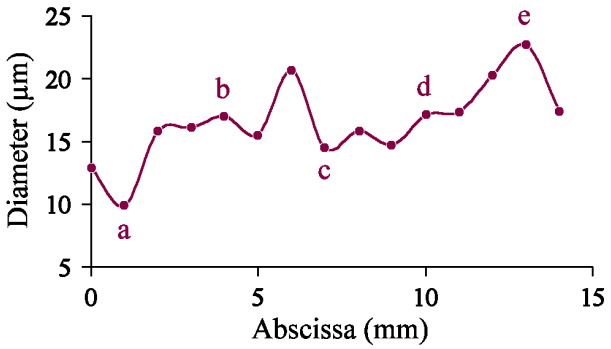

Fig. 9. Diameter profile of the fiber presented in figure 8 (the letters correspond respectively to the five micrographs)

6 Mechanical properties and fiber size

In order to check if the scattering of the mechanical properties could be explained by the scattering of the fiber profiles, forty fibers have been tensile tested as previously described. Their "fiber diameter" and thus their mechanical properties have been evaluated from two methods. In the first one, the diameter corresponds to the mean value of three optical measurements taken at different locations along the fiber before tensile testing. In the second one the diameter is measured by SEM analysis near the location of the rupture after the tensile test. The diameters measured from the two methods are compared in figure 10 and the mean values obtained for the mechanical properties are given in table 2.

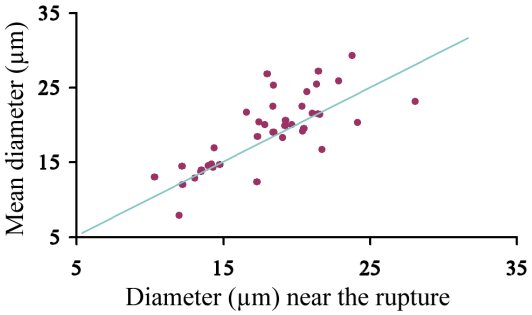

Fig. 10. Mean optical diameter before testing versus the diameter near the rupture

Table 2. Mean characteristics of the fibers according to the method used for their calculations

Method	d (µm)	E (GPa)	σ_r (MPa)
1st	19.1 ± 4.9	52 ± 17	915 ± 354
2nd	18.1 ± 3.9	55 ± 17	995 ± 345

It seems reasonable to suppose that the highest mechanical solicitation of a flax fiber should be at a location where the fiber diameter is the smallest. Thus the mean optical method should systematically overestimate the diameter of the rupture cross-section in comparison to the diameter measured near the rupture. It can be seen in figure 10 that this is not true: the experimental points are dispersed around a straight line of slope 1. This is confirmed by plotting the difference between the Young's moduli E_M and E_R calculated respectively from the first and second methods as a function of the diameter measured near the rupture (figure 11). From the mean optical diameter, one should always underestimate the value of the Young's modulus in comparison to the other method. Contrarily to what had been expected, it can be seen in figure 11 that the difference between the two moduli E_M-E_R is not necessarily negative. Then, the prediction of the mechanical behavior of a fiber seems out of reach from its diameter profile.

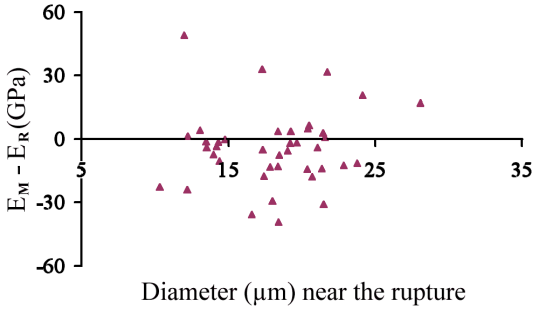

Fig. 11. Difference between the two calculated Young's moduli as a function of the fiber diameter measured near the rupture point

From the results presented in table 2, it appears that the method used to calculate the fiber diameter does not affects markedly neither the mean values of the mechanical properties nor their scattering. This scattering is clearly visible on the figures 12 and 13 where the mechanical properties have been reported as a function of the fiber diameter measured by the two methods.

Further investigations have been made on the fibers for which the complete diameter profile had been previously determined: they have been tensile tested and their diameter near the surface of rupture has been measured. It has then been observed that these fibers did not automatically fail at a location corresponding to the smallest diameter.

Consequently, it is supposed that the structural defects play a more important role in determining the location of the fiber failure than the fiber dimensions. The scattering of the mechanical properties cannot then be explained by the fiber size variations.

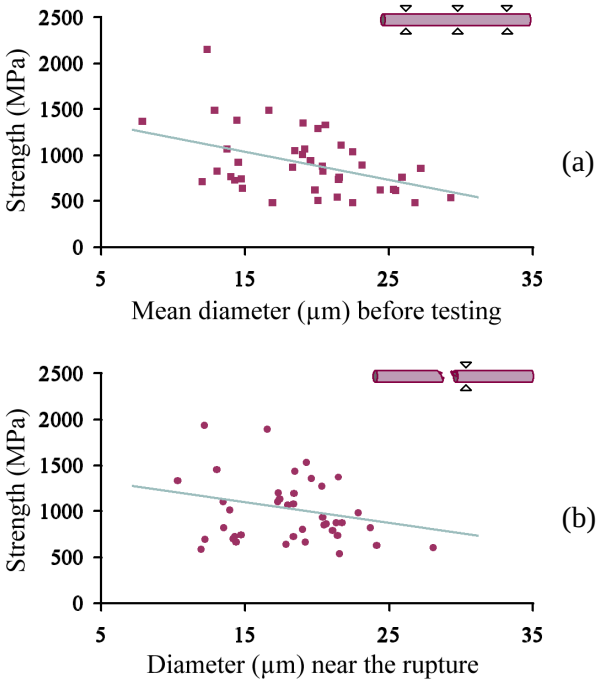

Fig. 12. Strength versus fiber diameter using the two methods described in the text

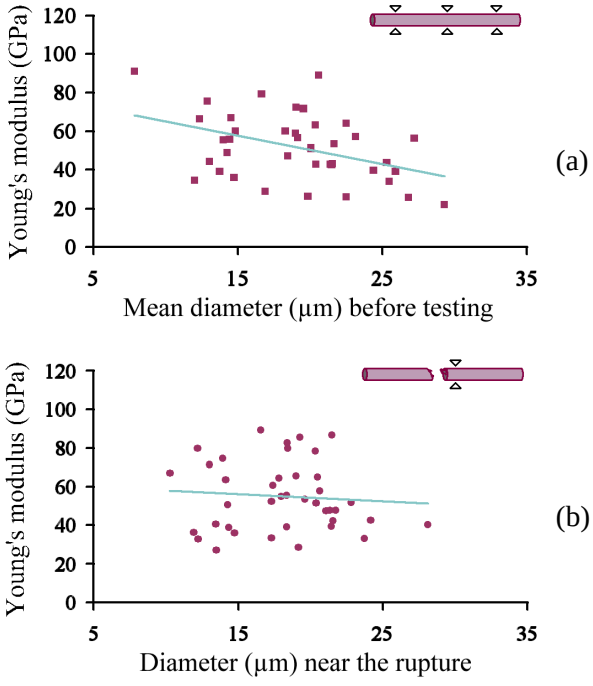

Fig. 13. Young's modulus versus fiber diameter using the two methods described in the text

In spite of the scattering of the results, a downward trend is clearly identified for the strength and the Young's modulus when the fiber size increases (figures 12 and 13).

Concerning the fiber strength, the two plots presented in figures 12a and 12b exhibit almost the same decreasing slope whatever the method of determination of diameter is (the second method only reduces the regression slope of 30%). Since the strength is directly correlated to the amount of defects in the tensile tested material, it is understandable that the larger the fiber, the higher the amount of defects, the higher the probability of rupture and thus the smaller the failure stress.

Contrarily to the strength, the Young's modulus should not depend on the fiber diameter. The modulus obtained from the average of optical measurements appears to be size-dependent (figure 13a) while the other one obtained from one measure in the vicinity of the rupture varies hardly with the fiber size (figure 13b). The slope of the regression line is found fourfold smaller in the second case than in the first one. Even if the large scattering of the results prevents from highlighting it more clearly, it seems that the decrease of the Young's modulus as a function of the fiber size can be ascribed to the size determination method.

7 Conclusion

Three main characteristics of the flax fiber tensile behavior have been studied along this work by taking into account the specific morphology of these fibers.

The first one is the non-linearity of the beginning of the tensile stress-strain curve. This departure from a linear behavior has been explained by a visco-elasto-plastic deformation of the amorphous polymers within the fiber together with a progressive alignment of its cellulose microfibrils with the tensile axis. A quantitative relationship has been proposed between the initial microfibril angle and the deformation corresponding to the realignment of the cellulose microfibrils. This explanation has been confirmed by further tensile tests carried out on cotton fibers.

The second one is the scattering of the experimental results. This scattering has been tentatively explained on the basis of the huge diameter variations observed by SEM along the profiles of the flax fibers. The mean diameter used for the calculations of the mechanical properties has then been replaced by a fiber diameter measured near the rupture location, but this correction had no effect on the scattering of mechanical properties. The structural defects probably play a more important role in the fiber failure than the fiber dimensions.

The third one is the decrease of the mechanical properties (Young's modulus and strength) as a function of the fiber size. By replacing the mean fiber diameter by the fiber diameter measured near the rupture, the downward trend of the Young's modulus as a function of the fiber size almost disappears.

Acknowledgments

The authors are grateful to the "Réseau Inter-Régional Matériaux Polymères, Plasturgie du Grand Bassin Sud-Parisien" for their financial support.

References

[1] Bert F. ITL, presentation to the Région Haute-Normandie, Rouen, 2007.

[2] Fédération de l'Industrie du verre. http://www.vgi-fiv.be/media/download/StatFIV.pdf. 2006

[3] Mukherjee P.S. and Satyanarayana K.G. "An empirical evaluation of structure-porpery relationships in natural fibres and their fracture behaviour". *Journal of Materials Science*, Vol. 21, pp. 4162-4168, 1986.

[4] Bos H.L. and Donald A.M. "*In situ* ESEM study of the deformation of elementary flax fibres". *Journal of Materials Science*, Vol. 34, pp. 3029-3034, 1999.

[5] Wang H.H., Drummond J.G., Reath S.M., Hunt K. and Watson P.A. "An improved fibril angle measurement method for wood fibres". *Wood Science and Technology, Vol. 34, pp. 493-503, 2001.*

[6] Batra S.K. "*Handbook of fibre chemistry*". Lewin M. and Pearce E.M. (eds), Marcel Dekker, pp. 505-575, 1998.

[7] Charlet K., Baley C., Morvan C., Jernot J.P., Gomina M. and Bréard J. "Characteristics of Hermès flax fibres as a function of their location in the stem and properties of the derived unidirectional composites". *Composites: Part A*, in press, 2007.

[8] Charlet K., Morvan C., Bréard J., Jernot J.P. and Gomina M. "Etude morphologique d'un composite naturel – La fibre de lin". *Revue des Composites et des Matériaux Avancés*, Vol. 16, pp. 11-24, 2006.

[9] Baley C. "Analysis of the flax fibres tensile behaviour and analysis of the tensile stiffness increase". *Composites: Part A*, Vol. 33, pp. 939-948, 2002.

[10] Nechwatal A., Mieck K.P. and Reuβmann T. "Developments in the characterization of natural fibre properties and in the use of natural fibres for composites". *Composites Science and Technology*, Vol. 63, pp. 1273-1279, 2003.

[11] Lilholt H. and Lawther J.M. "*Comprehensive Composite Materials*". Kelly A. and Zweben C. (eds), Elsevier, Vol. 1, pp. 303-325, 2000.

[12] Joffe R., Andersons J. and Wallström L. "Strength and adhesion characteristics of elementary flax fibres with different surface treatments". *Composites: Part A*, Vol. 34, pp. 603-612, 2003.

[13] Andersons J., Sparnins E., Joffe R. and Wallström L. "Strength distribution of elementary flax fibres". *Composites Science and Technology*, Vol. 65, pp. 693-702, 2005.

[14] Zafeiropoulos N.E. and Baillie C.A. "A study of surface treatments on the tensile strength of flax fibres: Part II. Application of Weibull statistics". *Composites: Part A*, Vol. 38, pp. 629-638, 2007.

[15] Salmén L.. "Micromechanical understanding of cell-wall structure". *Comptes Rendus Biologies*, Vol. 327, pp. 873-880, 2004.

[16] Wild P.M., Provan J.W., Pop S. and Guin R. "The effects of cyclic axial loading of single wood pulp fibers at elevated temperature and humidity". *TAPPI Journal*, Vol. 82, No. 4, pp. 209-215, 1999.

[17] Bossuyt V. "Etude de la structure et des propriétés mécaniques de la fibre de lin", *Thesis*, Université de Lille, France, 1941.

[18] Fenwick K.M., Jarvis M.C. and Apperley D.C. "Estimation of polymer rigidity in cell walls of growing and nongrowing celery collenchyma by solid-state nuclear magnetic resonance in vivo", *Plant Physiology*, Vol. 115, pp. 587-592, 1997.

[19] Busnel F. "Contribution à l'étude des matériaux composites à matrice organique renforcés par des fibres de lin – Influence des traitements chimiques sur la liaison interfaciale fibre/matrice", *Thesis*, Université de Bretagne Sud, France, 2006.

[20] Krakhmalev V.A. and Paiziev A.A. "Spiral structures of cotton fiber". *Cellulose*, Vol. 13, pp. 45-52, 2006.

[21] Wakelyn P.J., Bertoniere N.R., French A.D., Zeronian S.H., Nevell T.P., Thibodeaux D.P., Blanchard E.J., Calamari T.A., Triplett B.A., Bragg C.K., Welch C.M., Timpa J.D. and Goynes W.R. "*Handbook of fiber Chemistry*". M. Lewin and E.M. Pearce (eds), pp. 577-715, 1998.